THE JOURNAL OF PHYSICAL CHEMISTRY A

Article

Cite This: J. Phys. Chem. A 2018, 122, 4882−4893

pubs.acs.org/JPCA

Toward High-Level Theoretical Studies of Large Biodiesel Molecules: An ONIOM [QCISD(T)/CBS:DFT] Study of the Reactions between Unsaturated Methyl Esters ($C_nH_{2n-1}COOCH_3$) and Hydrogen Radical

Lidong Zhang,[†] Qinghui Meng,[†,‡] Yicheng Chi,[‡] and Peng Zhang*[,‡]

[†]National Synchrotron Radiation Laboratory, University of Science and Technology of China, Hefei, China

[‡]Department of Mechanical Engineering, The Hong Kong Polytechnic University, Hung Hom, Hong Kong, China

Supporting Information

ABSTRACT: A two-layer ONIOM[QCISD(T)/CBS:DFT] method was proposed for the high-level single-point energy calculations of large biodiesel molecules and was validated for the hydrogen abstraction reactions of unsaturated methyl esters that are important components of real biodiesel. The reactions under investigation include all the reactions on the potential energy surface of $C_nH_{2n-1}COOCH_3$ (n = 2−5, 17) + H, including the hydrogen abstraction, the hydrogen addition, the isomerization (intramolecular hydrogen shift), and the β-scission reactions. By virtue of the introduced concept of chemically active center, a unified specification of chemically active portion for the ONIOM (ONIOM = our own n-layered integrated molecular orbital and molecular mechanics) method was proposed to account for the additional influence of C═C double bond. The predicted energy barriers and heats of reaction by using the ONIOM method are in very good agreement with those obtained by using the widely accepted high-level QCISD(T)/CBS theory, as verified by the computational deviations being less than 0.15 kcal/mol, for almost all the reaction pathways under investigation. The method provides a computationally accurate and affordable approach to combustion chemists for high-level theoretical chemical kinetics of large biodiesel molecules.

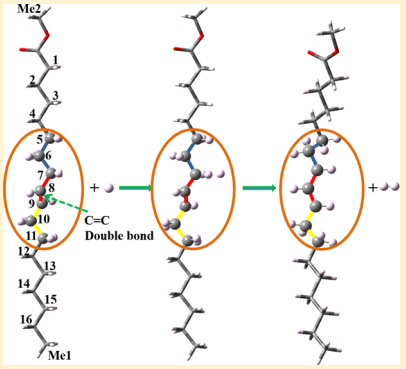

1. INTRODUCTION

Ever-increasing concerns about global energy security, environmental protection, and climate change have urged contemporary combustion researchers to study alternative fuels that are renewable and sustainable. Biodiesel is a promising alternative fuel owing to its many advantages such as renewability, domestic production, and lower pollutant emissions.[1] Its derivation from chemically reactive lipids (e.g., vegetable oil, soybean oil, and animal fat) with an alcohol through the trans-esterification process[2,3] leads to a mixture of saturated and unsaturated methyl and ethyl esters. The molecule of these esters usually contains 12 or more carbon atoms.[4,5]

Motivated by establishing high-fidelity, quantitatively accurate, detailed reaction mechanisms to promote the computer-aided design and optimization of practical combustion energy conversion devices, numerous studies have been conducted on the chemical kinetics of biodiesel combustion in the past decade.[6−11] The mechanism development of biodiesel, which contains diverse constituent molecules of large size, is however challenging, because biodiesel combustion produces a formidably complex reaction system involving approximately thousands of species and 10 times more reactions. As a result, surrogate fuels of smaller molecular sizes were extensively studied in recent years in the hope of imitating the combustion characteristics of real biodiesel. Small saturated methyl esters, particularly methyl butanoate, have been the focus of many experimental and theoretical studies.[12−16]

In consideration of the major components of biodiesel being unsaturated alkyl esters with mono- and multi-C═C bonds and that the presence of double bond(s) has a great influence on the ignition delay and the cetane number,[17] chemical kinetics of unsaturated biodiesel surrogate molecules have come to the attention of researchers recently. For small unsaturated esters, Sarathy et al.[18] compared methyl butanoate [$CH_3(CH_2)_2COOCH_3$] and methyl crotanoate [$CH_3CH{=}CHCOOCH_3$] and experimentally found that both molecules have similar reactivity, but the unsaturated one has a greater sooting tendency. Gail et al.[19] proposed a detailed reaction mechanism for methyl crotanoate oxidation based on the mechanisms developed for methyl butanoate. The experimental study on a blend of n-decane and methyl oleate [$CH_3(CH_2)_7CH{=}CH(CH_2)_7COOCH_3$] was conducted by Bax et al.[20] in a jet-stirred reactor and over a temperature range of 550−1100 K. Attributed to the presence of C═C double bond, a slightly lower reactivity was observed for the blend compared with that of the blend of n-decane and methyl palmitate [$CH_3(CH_2)_{14}COOCH_3$]. On the basis of the reaction mechanism for methyl

Received: March 9, 2018
Revised: May 2, 2018
Published: May 10, 2018

DOI: 10.1021/acs.jpca.8b02327
J. Phys. Chem. A 2018, 122, 4882−4893

decanoate oxidation, Herbinet et al.[21] developed detailed chemical kinetics mechanisms for methyl-5-decenoate [$CH_3(CH_2)_3CH{=}CH(CH_2)_3COOCH_3$] and methyl-9-decenoate [$CH_2{=}CH(CH_2)_7COOCH_3$] and validated the mechanisms against the jet-stirred reactor experiments for rapeseed oil methyl esters oxidation. For developing the reaction mechanism for methyl oleate [$CH_3(CH_2)_7CH{=}CH(CH_2)_7COOCH_3$], Naik et al.[22] adopted the existing reaction classes and the semiempirical rules for reaction rate constant and supplemented the reaction classes associated with methyl esters. On the basis of the autoignition database of small unsaturated esters,[23−26] extensive studies have been also conducted to investigate the effects of C=C double bonds on the reactivity and products of medium-sized unsaturated esters.[27−30]

In spite of these worthy studies, we noted that few theoretical chemical kinetics studies have been performed for unsaturated large ester molecules. Evidently, accurate theoretical prediction of energy barriers and heats of reaction for key reaction pathways is crucial for the construction of detailed reaction mechanism, whose uncertainty is critically influenced by the rate constants and thermodynamics data.[31] Several high-level post-Hartree−Fock methods together with large basis sets have been sufficiently demonstrated for their computational accuracy and affordability for relatively small molecular systems.[11] For example, the coupled cluster theory, with single and double excitations, and a quasi-perturbative treatment of connected triple excitations [CCSD(T)], with an extrapolation to complete basis set (CBS), yields the predictions of barrier height and reaction energy with uncertainties less than 1.0 kcal/mol[31] in the systems without strong multireference characteristics; otherwise, the post-CCSD(T) methods such as CCSDT(Q) may be needed. The quadratic configuration interaction with singles, doubles, and perturbative inclusion of triples, and with an extrapolation to complete basis set [QCISD(T)/CBS] usually has uncertainties ∼1.0 kcal/mol, which can further be reduced to 0.6 kcal/mol with a bond additivity correction.[32] These high-level methods are, however, computationally infeasible for large molecules containing more than 9 or 10 carbon atoms.

Recognizing that few attempts have been made to produce high-level thermochemical and kinetic data for larger esters and urged by the need to develop methodologies for high-level chemical kinetics of larger biodiesel molecules, Zhang and Zhang[11] proposed a two-layer ONIOM (ONIOM = our own *n*-layered integrated molecular orbital and molecular mechanics) method,[33] in which the QCISD(T)/CBS method is used for the high layer and the B3LYP-favor density functional theory (DFT) method for the low layer. The ONIOM [QCISD(T)/CBS:DFT] method was systematically validated by calculating the energy barriers and the heats of reaction of the hydrogen abstraction reactions of saturated alkyl esters, $C_nH_{2n+1}COOC_mH_{2m+1}$ (n = 1−5, m = 1 or 2), by a hydrogen radical, which are among the key reactions in combustion of alkyl esters. The calculated energies were found to be almost identical to those QCISD(T)/CBS energies, with the discrepancies being less than 0.1 kcal/mol for all the tested cases. The ONIOM-[QCISD(T)/CBS:DFT] method was subsequently applied to larger systems, such as methyl decanoate (MD, n = 9, m = 1) and methyl heptadecanoate (n = 15, m = 1), and used to examine the widely used Evans−Polanyi relations, which are however insufficiently accurate for high-level chemical kinetics because of the large uncertainty of ±2.0 kcal/mol.

In the present study, we further developed and validated the ONIOM[QCISD(T)/CBS:DFT] method for the reactions between hydrogen radical and unsaturated methyl esters $C_nH_{2n-1}COOCH_3$ (n = 2−5) and subsequently applied it to methyl oleate (n = 17). This study is considered a significant extension and complement of Zhang and Zhang's previous work[11] for the following reasons. First, the ONIOM[QCISD-(T)/CBS:DFT] method would not be considered practically useful until its applicability is verified for not only saturated esters but also unsaturated esters, given that the latter are important components of real biodiesel. Second, the specification of chemically active portion (CAP) for the ONIOM method needs additional theoretical consideration to account for the influence of C=C double bond. Third, the energetically favored reactions between hydrogen radical and $C_nH_{2n-1}COOCH_3$ are not limited to hydrogen abstraction reactions. Instead, hydrogen radical can be added to the double bond to form a radical $C_nH_{2n}COOCH_3$, which subsequently undergoes isomerization (intramolecular hydrogen shift) reactions and β-scission reactions. The emergence of these reactions substantially increases the theoretical and computational complexity of the present study, as shall be expatiated shortly in the following sections.

2. COMPUTATIONAL METHODOLOGY

2.1. Potential Energy Surfaces and ONIOM Energies. Following the previous study by Zhang and Zhang,[11] the Becke three-parameter functional and the Lee−Yang−Parr correlation functional (B3LYP) with the 6-311++G(d,p) basis set[34,35] was used in the geometry optimization and the calculation of vibrational frequencies for all stationary points on the potential energy surfaces of $C_nH_{2n-1}COOCH_3$ + H (n = 2−5, 17). To confirm the identified transition state, the intrinsic reaction path (IRC) was used to examine the connection of each local maxima to its local minima. Zero-point energy (ZPE) corrections were obtained from the B3LYP/6-311++G(d, p) vibrational frequencies.

To validate the calculated single-point energies by using the ONIOM[QCISD(T)/CBS:DFT] method, we employed the QCISD(T)/CBS energies, which are constructed by using the QCISD(T) energies with cc-pVDZ and cc-pVTZ basis sets, and the energies from the second-order Møller−Plesset theory correction (MP2) with cc-pVDZ, cc-pVTZ and cc-pVQZ basis sets. These energies were extrapolated to the complete basis set by using the following equation:[32]

$$\mathrm{E[QCISD(T)/CBS]} = \mathrm{E[QCISD(T)/CBS]_{DZ\rightarrow TZ}} + \{\mathrm{E[MP2/CBS]_{TZ\rightarrow QZ}} - \mathrm{E[MP2/CBS]_{DZ\rightarrow TZ}}\} \quad (1)$$

where

$$\mathrm{E[QCISD(T)/CBS]_{DZ\rightarrow TZ}} = \mathrm{E[QCISD(T)/TZ]} + \{\mathrm{E[QCISD(T)/TZ]} - \mathrm{E[QCISD(T)/DZ]}\} \times 0.4629 \quad (2)$$

$$\mathrm{E[MP2/CBS]_{TZ\rightarrow QZ}} = \mathrm{E[MP2/QZ]} + \{\mathrm{E[MP2/QZ]} - \mathrm{E[MP2/TZ]}\} \times 0.6938 \quad (3)$$

$$\mathrm{E[MP2/CBS]_{DZ\rightarrow TZ}} = \mathrm{E[MP2/TZ]} + \{\mathrm{E[MP2/TZ]} - \mathrm{E[MP2/DZ]}\} \times 0.4629 \quad (4)$$

In the previous studies on the isomerization and decomposition reactions of hydroxybutyl and butoxy radicals (C_4H_9O), the hydrogen abstraction and addition reactions of methyl butanoate [$CH_3(CH_2)_2COOCH_3$] by H and OH radicals,[27] and the

DOI: 10.1021/acs.jpca.8b02327
J. Phys. Chem. A 2018, 122, 4882−4893

hydrogen abstraction reaction of $C_nH_{2n+1}COOC_mH_{2m+1}$ (n = 0–2, m = 1 or 2) by H radical, the method (1) has been validated by comparing with the widely used the $[QCISD(T)/CBS]_{TZ\rightarrow QZ}$ method given by

$$E[QCISD(T)/CBS]_{TZ\rightarrow QZ} = E[QCISD(T)/QZ] + \{E[QCISD(T)/QZ] - E[QCISD(T)/TZ]\} \times 0.6938 \quad (5)$$

With the errors being less than 0.1 kcal/mol in all the tested cases, the QCISD(T)/CBS method (1) avoids the computationally expensive QCISD(T)/QZ calculations and thereby can be used in the present system up to n = 5, beyond which the method becomes computationally formidable and should be replaced by the ONIOM[QCISD(T)/CBS:DFT] method.

The ONIOM energy of the whole system was obtained by using the low-level energy of the system with the available correction for the energy difference of CAP between the high level and the low level:

$$E^{ONIOM}[High/Low] = E^{Low}(R) + E^{High}(CAP) - E^{Low}(CAP) \quad (6)$$

Using the B3LYP/6-311++G(d,p) method for the low level and the QCISD(T)/CBS method (1) for the high level, we have the ONIOM[QCISD(T)/CBS:DFT] energy given by

$$E^{ONIOM}[QCISD(T)CBS:DFT] = E^{ONIOM} \times [QCISD(T)/CBS:DFT]_{DZ\rightarrow TZ} + \{E^{ONIOM}[MP2/CBS:DFT]_{TZ\rightarrow QZ} - E^{ONIOM}[MP2/CBS:DFT]_{DZ\rightarrow TZ}\} \quad (7)$$

where

$$E^{ONIOM}[QCISD(T)/CBS:DFT]_{DZ\rightarrow TZ} = E^{ONIOM}[QCISD(T)/TZ:DFT] + \{E^{ONIOM}[QCISD(T)/TZ:DFT] - E^{ONIOM} \times [QCISD(T)/DZ:DFT]\} \times 0.4629 \quad (8)$$

$$E^{ONIOM}[MP2/CBS:DFT]_{TZ\rightarrow QZ} = E^{ONIOM} \times [MP2/QZ:DFT] + \{E^{ONIOM}[MP2/QZ:DFT] - E^{ONIOM}[MP2/TZ:DFT]\} \times 0.6938 \quad (9)$$

$$E^{ONIOM}[MP2/CBS:DFT]_{DZ\rightarrow TZ} = E^{ONIOM} \times [MP2/TZ:DFT] + \{E^{ONIOM}[MP2/TZ:DFT] - E^{ONIOM}[MP2/DZ:DFT]\} \times 0.4629 \quad (10)$$

The ZPE-corrected energy barrier (referred to as EB hereinafter) of a reaction is the difference between the energies (E^{ONIOM}[QCISD(T)/CBS:DFT] + ZPE) of the reactant(s) and the transition state:

$$EB = (E^{ONIOM}[QCISD(T)/CBS:DFT] + ZPE)_{TS} - (E^{ONIOM}[QCISD(T)/CBS:DFT] + ZPE)_{reactants} \quad (11)$$

The ZPE-corrected heats of reaction (referred to as HR hereinafter) of a reaction is the change between the energy (E^{ONIOM}[QCISD(T)/CBS:DFT] + ZPE) of the reactant(s) and the product(s):

$$HR = (E^{ONIOM}[QCISD(T)/CBS:DFT] + ZPE)_{products} - (E^{ONIOM}[QCISD(T)/CBS:DFT] + ZPE)_{reactants} \quad (12)$$

All the calculations in the present study were performed by the Gaussian program.[36]

2.2. Chemically Active Portion (CAP). *2.2.1. General Description.* The present ONIOM[QCISD(T)/CBS:DFT] method divides a reaction system into two layers, which are treated at different theoretical levels. The high-level layer, also known as the chemically active portion (denoted by CAP hereinafter), is treated at the QCISD(T)/CBS level, while the low-level layer is at the B3LYP/6-311++G(d, p) level. The method uses hydrogen atoms as link atoms to saturate the dangling bonds, and functional groups are always included in the same layer. The accuracy of the choice of link atoms has been substantiated for saturated alkyl ester systems[11] and will be further verified for unsaturated methyl ester systems in the present study.

A crucial issue of employing an ONIOM method is to specify the CAP to balance the computational accuracy and cost. In the previous study on the hydrogen abstraction reactions of saturated alkyl esters by hydrogen radical, the CAP consists of the CH_2 (or CH_3) group under hydrogen attack and the neighboring CH_2 (or CH_3, C═O, C−O) groups. To determine the minimally required CAP with satisfactory calculation accuracy, Zhang and Zhang[11] specified a CAP by two integers N_1 and N_2, which are the numbers of the main-chain non-hydrogen atoms on each side of the CH_2 (or CH_3) under hydrogen attack. Consequently, the total number of non-hydrogen atoms included in the CAP(N_1, N_2) is generally $N_1 + N_2 + 1$, which dominantly determines the computational cost of the ONIOM method.

In the previous study, systematical tests for all the possible combinations of (N_1, N_2) were conducted on the systems of $C_5H_{11}COOCH_3$ + H and C_9H_{20} + H, the largest systems that were computationally affordable by the authors for the validation at the QCISD(T)/CBS level. The test results suggest that CAP(2,2) is minimally required for the ONIOM method to accurately predict EB and HR with the errors being less than 0.1 kcal/mol compared with the QCISD(T)/CBS method. Furthermore, the specification of CAP(2,2) must be done to maintain the integrity of the functional group: the carbonyl C atom, the alkoxy O atom, and the carbonyl O atom must be all included in CAP(2,2), if any one of these atoms is included. Consequently, we believed that CAP(2,2) is sufficiently large for the present unsaturated methyl ester systems. As will be seen in the present calculations, CAP(2,2) indeed remains a satisfactory choice for the unsaturated methyl ester reaction systems under consideration.

Compared with the hydrogen abstraction reactions of saturated alkyl esters, the specification of CAP for the reactions between hydrogen radical and unsaturated methyl esters ($C_nH_{2n-1}COOCH_3$) is more complex due to the presence of C═C double bond and therefore requires specific discussion according to the reaction type. However, it will be seen shortly that a generalization of CAP(2,2)—consistent to its previous version—can be obtained by introducing a concept of chemically active center (CAC) to account for the conjugation influence of C═C double bond.

Methyl oleate [$CH_3(CH_2)_7CH$═$CH(CH_2)_7COOCH_3$] with one double bond located in the middle of the long carbon chain is

DOI: 10.1021/acs.jpca.8b02327
J. Phys. Chem. A 2018, 122, 4882−4893

one of most common components of rapeseed biodiesel with a mass ratio being ~59.9%.[22,37] It will be used as a representative unsaturated methyl ester for illustrating the specifications of CAP in the following subsections.

2.2.2. CAP(2,2) for Hydrogen Addition Reactions. For methyl oleate as shown in Figure 1, the indices 1−16 denote the CH_2 (or CH) groups from the one adjacent to the ester group to the one at the far end of the alkyl chain. The double bond C═C is located between the No. 8 and No. 9 CH groups. Me1 denotes the methyl group in the alkyl chain, and Me2 indicates the one connected to the ester group. As a representative example, a hydrogen atom is added to the No. 9 CH group, resulting in the reaction $CH_3(CH_2)_7CH{=}CH(CH_2)_7COOCH_3 + H\cdot \rightarrow CH_3(CH_2)_7CH{=}CHCH\cdot(CH_2)_6COOCH_3 + H_2$. For the addition reaction of a hydrogen atom to the No. 8 CH group, the specification of CAP(2,2) is similar and straightforward.

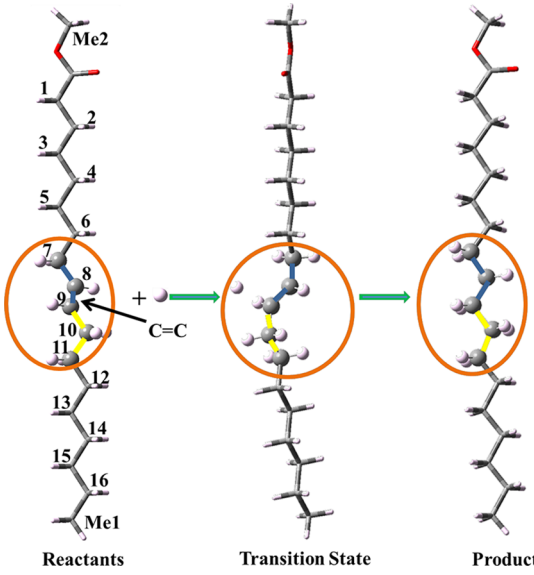

Figure 1. Illustration of the ONIOM[QCISD(T)/CBS:DFT]/CAP-(2,2) method for a representative hydrogen addition reaction of methyl oleate, $CH_3(CH_2)_7CH{=}CH(CH_2)_7COOCH_3 + H\cdot \rightarrow CH_3(CH_2)_8CH\cdot(CH_2)_7COOCH_3$. The indices 1−16 denote CH_2 (or CH) groups from the one adjacent to the ester group to the one at the far end of the alkyl chain. The double bond C═C is located between the No. 8 and No. 9 CH groups. Me1 denotes the methyl group in the alkyl chain, and Me2 indicates the one connected to the ester group. CAC consists of the No. 9 CH group under the attack of an H atom. CAP(2,2) represents the CAP consisting of the CAC, the No. 10 and No. 11 CH_2 groups on the one side of the CAC, and the No. 8 CH group and the No. 7 CH_2 group on the other side of the CAC.

Similar to that in the previous study for hydrogen abstraction reactions, the CAP(2,2) for the hydrogen addition reaction consists of three parts: the No. 9 CH group under the hydrogen attack, the No. 10 and No. 11 CH_2 groups on the one side of the No. 9 CH group, and the No. 8 CH group and the No. 7 CH_2 group on the other side of the No. 9 CH group. For the consistency and conciseness of the present theoretical description, we define the No. 9 CH group under hydrogen attack as the CAC of the CAP for the reason to be manifested shortly. Consequently, the CAP(2,2) can be simply specified as to include the CAC and two CH_2 (or CH) groups on each of its sides.

2.2.3. CAP(2,2) for Hydrogen Abstraction Reactions. For the hydrogen abstraction reactions of methyl oleate, the CAP(2,2) must be specified according to the site of CH_2 (or CH_3) group under hydrogen attack. If the abstracted hydrogen atom is from neither No. 7 nor No. 10 CH_2 groups, the CAC is the CH_2 (or CH_3) group under attack, and the corresponding CAP(2,2) is similar to that specified in the previous study.

As the CH_2 groups of No.7 or No.10 are located at the β position of the C═C double bond, the electrons in a σ orbital interact with those in an adjacent π orbital, producing an extended molecular orbital. Unsaturated methyl esters with C═C bond are stabilized with the increased electron delocalization associated with the hyperconjugation effect. Moreover, ally radicals with strong conjugation effect are produced when hydrogen abstraction reactions occur at either No.7 or No.10 CH_2 group that locates at the β sites of the C═C bond. Thus, the CAC must be enlarged to include the C═C double bond because of the conjugation effect of the double bond. Figure 2 shows the hydrogen abstraction from the No. 7 CH_2 group, $CH_3(CH_2)_7CH{=}CH(CH_2)_7COOCH_3 + H\cdot \rightarrow CH_3(CH_2)_7CH{=}CHCH\cdot(CH_2)_6COOCH_3 + H_2$, as a representative case. The CAC consists of the No. 7 CH_2 group under hydrogen attack and the adjacent C═C double bond (i.e., the No. 8 and No. 9 CH groups). Consequently, the CAP(2,2) consists of the CAC, the No. 5 and No. 6 CH_2 groups on the one side of the CAC, and No. 10 and No. 11 CH_2 groups on the other side of the CAC.

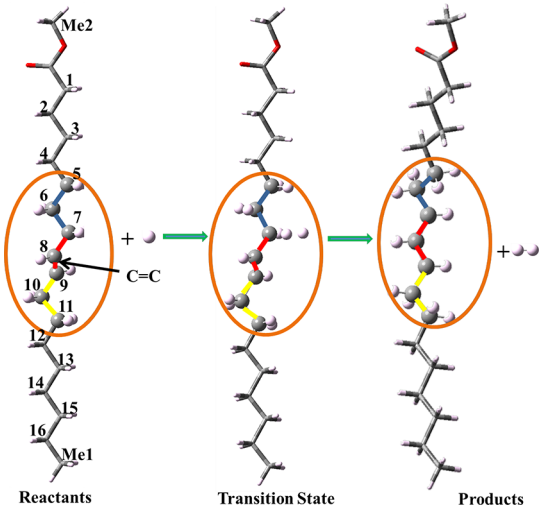

Figure 2. Illustration of the ONIOM[QCISD(T)/CBS:DFT]/CAP-(2,2) method for a representative hydrogen abstraction reaction of methyl oleate, $CH_3(CH_2)_7CH{=}CH(CH_2)_7COOCH_3 + H\cdot \rightarrow CH_3(CH_2)_7CH{=}CHCH\cdot(CH_2)_6COOCH_3 + H_2$. The indices 1−16 denote the CH_2 (or CH) groups from the one adjacent to the ester group to the one at the far end of the alkyl chain. The double bond C═C is located between the No. 8 and No. 9 CH groups. Me1 denotes the methyl group in the alkyl chain, and Me2 denotes the one connected to the ester group. CAC consists of the C═C double bond (i.e., the No. 8 and No. 9 CH groups) and the adjacent No. 7 CH_2 group under hydrogen attack. CAP(2,2) represents the CAP consisting the CAC, the No. 5 and No. 6 CH_2 groups on the one side of the CAC, and No. 10 and No. 11 CH_2 groups on the other side of the CAC.

Evidently, by virtue of the defined CAC, the CAP(2,2) for all the hydrogen abstraction reactions can be consistently specified as consisting of the CAC and two CH_2 (or CH, CH_3) groups on each side of the CAC.

DOI: 10.1021/acs.jpca.8b02327
J. Phys. Chem. A 2018, 122, 4882−4893

2.2.4. CAP(2,2) for Isomerization Reactions. On the potential energy surface (PES) of $C_nH_{2n-1}COOCH_3$ + H, the hydrogen addition reactions are followed by the isomerization and β-scission reactions. These isomerization reactions are characterized by the intramolecular hydrogen shift from a CH_2 (or CH_3) group to a CH group. Apparently, both groups between which a hydrogen atom shifts must be considered chemically active in such a reaction. Consequently, the CAP should contain two CACs: one is the CH_2 (or CH_3) group yielding the hydrogen atom, and the other is the CH group receiving the hydrogen atom. As a result, the CAP(2,2) is enlarged to include the two CACs and the two CH_2 (or CH, CH_3) groups on the each side of each CAC, yielding to totally 10 non-hydrogen atoms in a nondegenerate case.

Figure 3 illustrates a representative isomerization reaction of the methyl oleate radical (the product shown in Figure 1),

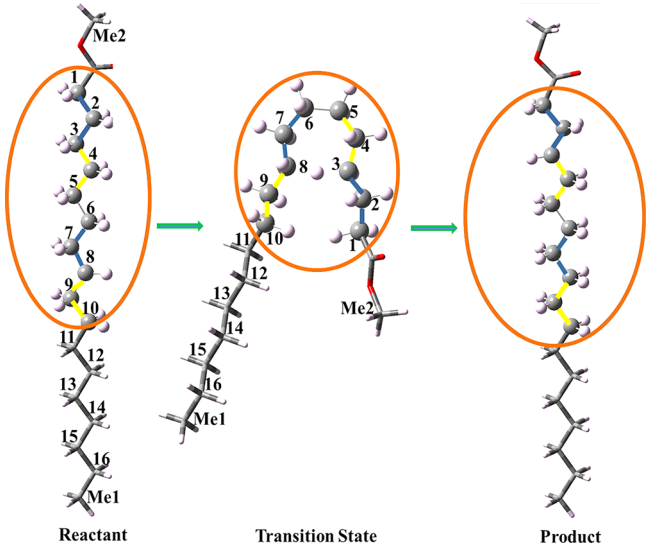

Figure 3. Illustration of the ONIOM[QCISD(T)/CBS:DFT]/CAP-(2,2) method for a representative isomerization (intramolecular hydrogen-shift) reaction of the methyl oleate radical (the product shown in Figure 1), $CH_3(CH_2)_8CH{\cdot}(CH_2)_7COOCH_3 \rightarrow CH_3(CH_2)_{13}CH{\cdot}(CH_2)_2COOCH_3$. The indices 1−16 denote the CH_2 (or CH) groups from the one adjacent to the ester group to the one at the far end of the alkyl chain. Me1 denotes the methyl group in the alkyl chain, and Me2 indicates the one connected to the ester group. CACs consist of the No. 3 CH_2 group yielding the hydrogen atom and the No. 8 CH group receiving the hydrogen atom. CAP(2,2) represents the CAP consisting of the CACs and the neighboring CH groups, which coincidentally include all the atoms within the 10-member ring.

$CH_3(CH_2)_8CH{\cdot}(CH_2)_7COOCH_3 \rightarrow CH_3(CH_2)_{13}CH{\cdot}(CH_2)_2COOCH_3$, where a hydrogen atom of the No. 3 CH_2 group shifts to the No. 8 CH group through a seven-member-ring transition state. The indices 1−16 denote the CH_2 (or CH) groups from the one adjacent to the ester group to the one at the far end of the alkyl chain. Me1 denotes the methyl group in the alkyl chain, and Me2 denotes the one connected to the ester group. The CACs are the No. 3 CH_2 group yielding the hydrogen atom and the No. 8 CH group receiving the hydrogen atom. The CAP(2,2) consists of the CACs, the four neighboring groups (No. 1 and No. 2, No. 4 and No. 5) of the No. 3 CH_2 group (the first CAC), and the four neighboring groups (No. 6 and No. 7, No. 9 and No. 10) of the No. 8 CH group (the second CAC).

For the case shown in Figure 3, the CAP(2,2) containing 10 non-hydrogen atoms coincidentally includes all the six carbon atoms within the seven-member-ring transition-state structure. For the isomerization reactions considered in the present investigation, this is the largest CAP(2,2) whose ring-structure transition state can be computed at the level of QCISD(T)/CBS. For any other cases where the transition state forms a larger multiple-member-ring structure, the transition state must be computed at different levels of theory. This may cause a relatively larger computational error but is beyond the present computational capability for validation.

2.2.5. CAP(2,2) for β-Scission Reactions. In general, the CAC for a β-scission reaction consists of the radical site and its adjacent α and β groups. The corresponding CAP(2,2) consists of the CAC and two neighboring groups on each side of the CAC. Figure 4 illustrates a representative β-scission reaction of the

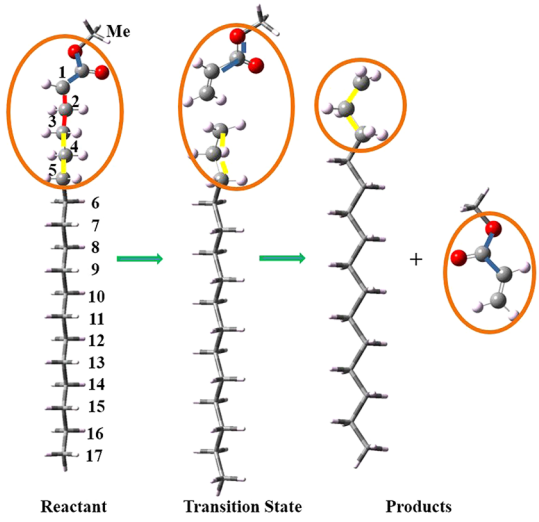

Figure 4. Illustration of the ONIOM[QCISD(T)/CBS:DFT]/CAP-(2,2) method for a representative β-scission reaction of the methyl oleate radical (the product shown in Figure 3), $CH_3(CH_2)_{15}CH{\cdot}COOCH_3 \rightarrow CH_3(CH_2)_{13}CH_2{\cdot} + H_2C{=}CHCOOCH_3$. The indices 1−16 denote the CH_2 (or CH) groups from the one adjacent to the ester group to the one at the far end of the alkyl chain. Me1 denotes the methyl group in the alkyl chain, and Me2 indicates the one connected to the ester group. The CAC consists of the No. 1 CH group and the No. 2 and No. 3 CH_2 groups involved in the β-scission. CAP(2,2) represents the CAP consisting of the CAC, the No. 4 and No. 5 CH_2 groups on the one side of the CAC, and the ester group on the other side of the CAC.

methyl oleate radical (the product of the reaction shown in Figure 3), $CH_3(CH_2)_{15}CH{\cdot}COOCH_3 \rightarrow CH_3(CH_2)_{13}CH_2{\cdot} + H_2C{=}CHCOOCH_3$, which is one of the most energetically favorable reaction channels on the PES of $C_{17}H_{33}COOCH_3$ + H. The indices 1−16 denote the CH_2 (or CH) groups from the one adjacent to the ester group to the one at the far end of the alkyl chain. Me1 denotes the methyl group in the alkyl chain, and Me2 indicates the one connected to the ester group. The CAC consists of the No. 1 CH group and the No. 2 and No. 3 CH_2 groups involved in the β-scission. The CAP(2,2) is composed of the CAC, the No. 3 and No. 4 CH_2 groups on the one side of the CAC, and the ester group on the other side of the CAC.

3. RESULTS AND DISCUSSION

3.1. Validation of ONIOM Energies of $C_nH_{2n-1}COOCH_3$ + H (n = 2−5). *3.1.1. Hydrogen Addition and Abstraction Reactions.* To validate the present ONIOM[QCISD(T)/CBS:DFT] method with the defined CAP (2,2), the calculated

DOI: 10.1021/acs.jpca.8b02327
J. Phys. Chem. A 2018, 122, 4882−4893

Table 1. Calculated EB and HR for $C_nH_{2n-1}COOCH_3$ + H (n = 2−5) with the ONIOM[QCISD(T)/CBS:DFT] and QCISD(T)/CBS Methods[a]

	k = Me2	k = 1	k = 2	k = 3	k = Me1	k = 4	k = 5
n = 2, l = 1	10.50(10.50)/	3.67(3.69)/	1.43(1.47)/				
	−5.30(−5.30)	−32.49(−32.43)	−40.13(−40.16)				
n = 3, l = 1	10.31(10.32)/	3.15(3.19)/	2.89(2.95)/		7.42(7.47)/		
	−5.45(−5.52)	−31.38(−31.38)	−35.65(−35.63)		−17.95(−17.92)		
n = 3, l = 2	10.56(10.50)/	4.85(4.90)/	3.67(3.70)/	1.41(1.36)/			
	−5.17(−5.26)	−22.24(−22.28)	−33.29(−33.28)	−35.84(−35.74)			
n = 4, l = 1	10.27(10.28)/	3.21(3.22)/	2.75(2.81)/	5.28(5.35)/	10.57(10.64)/		
	−5.49(−5.56)	−31.62(−31.52)	−36.25(−36.23)	−21.89(−21.91)	−2.91(−2.83)		
n = 4, l = 2	10.52(10.43)/	4.44(4.49)/	2.56(2.60)/	2.84(2.77)/	7.15(7.23)/		
	−5.29(−5.39)	−23.07(−23.16)	−33.45(−33.44)	−32.83(−32.77)	−16.73(−16.65)		
n = 4, l = 3	10.45(10.41)/	7.35(7.32)/	6.03(6.12)/	3.70(3.69)/		1.24(1.17)/	
	−5.37(−5.43)	−9.99(−10.01)	−18.52(−18.44)	−32.40(−32.37)		−35.27(−35.22)	
n = 5, l = 1	10.22(10.23)/	3.29(3.18)/	3.20(3.20)/	5.32(5.38)/	10.38(10.29)/	8.27(8.24)/	
	−5.56(−5.64)	−31.50(−31.39)	−36.16(−36.13)	−21.32(−21.35)	−3.50(−3.47)	−5.90(−5.82)	
n = 5, l = 2	10.55(10.48)/	4.46(4.49)/	2.96(2.94)/	2.99(2.82)/	10.35(10.41)/	5.24(5.31)/-	
	−5.56(−5.64)	−23.00(−23.09)	−33.43(−33.47)	−33.20(−33.13)	−3.39(−3.33)	19.73(−19.69)	
n = 5, l = 3	10.41(10.37)/	7.37(7.37)/	5.65(5.73)/	2.69(2.99)/	7.16(7.16)/	2.93(2.83)/	
	−5.42(−5.49)	−9.87(−9.85)	−18.65(−18.59)	−32.66(−32.64)	−16.82(−16.79)	−32.39(−32.37)	
n = 5, l = 4	10.45(10.41)/	7.19(7.12)/	8.45(8.51)/	5.35(5.42)/		3.52(3.55)/	1.21(1.19)/
	−5.34(−5.41)	−10.28(−10.32)	−5.30(−5.30)	−19.26(−19.33)		−32.60(−32.53)	−35.14(−35.12)

[a]The notation l (= 1−4) denotes the possible location of C═C double bond from the closest to the farthest to the ester group, and k (= 1−5, Me1, Me2) denotes the group under hydrogen attack, where Me1 denotes the CH_3 in the alkyl chain and Me2 denotes the CH_3 connected to the alkoxy O atom. Each item in the table reads as EB by the ONIOM method (EB by the QCISD(T)/CBS method)/HR by the ONIOM method (HR by the QCISD(T)/CBS method). Empty cells correspond to those nonexistent reactions.

EB and HR for the addition and abstraction reactions of $C_nH_{2n-1}COOCH_3$ + H (n = 2−5) are presented in Table 1. All the possible locations of the C═C double bond and the hydrogen attack sites were considered for a systematical and comprehensive validation. The notation l (= 1−4) denotes the location of double bond from the closest to the farthest to the ester group, and k (= 1−5, Me1, and Me2) denotes the group under H attack. Me1 denotes the CH_3 in the alkyl chain, and Me2 denotes the CH_3 connected to the alkoxy O atom. The empty cells in Table 1 correspond to those nonexistent reactions.

It is seen from Table 1 that the predicted energies using the ONIOM and the QCISD(T)/CBS methods are in very good agreement. The EBs of hydrogen addition reactions are substantially smaller than those of H abstraction reactions as expected. For the hydrogen abstraction reactions at saturated sites, EBs of unsaturated esters are almost identical with that of saturated esters obtained previously,[11] while for the hydrogen abstraction at α sites of C═C, EBs are smaller due to the conjugation effect.

To facilitate the comparison between the ONIOM[QCISD(T)/CBS:DFT] and QCISD(T)/CBS energies for better perception, the differences (in absolute value) between EB[ONIOM] (or HR[ONIOM]) and EB[QCISD(T)/CBS] (or HR[QCISD(T)/CBS]) are depicted in Figure 5. It is seen that almost all the differences are less than 0.15 kcal/mol and that the majority of them are actually less than 0.1 kcal/mol, substantiating the accuracy of the present ONIOM method.

The only exceptional case is the EB for the hydrogen addition reaction (n = 5, l = 2, k = 3),

$$CH_3CH_2CH{=}CHCH_2COOCH_3 + H\cdot \rightarrow CH_3(CH_2)_2CH\cdot CH_2COOCH_3 \quad (13)$$

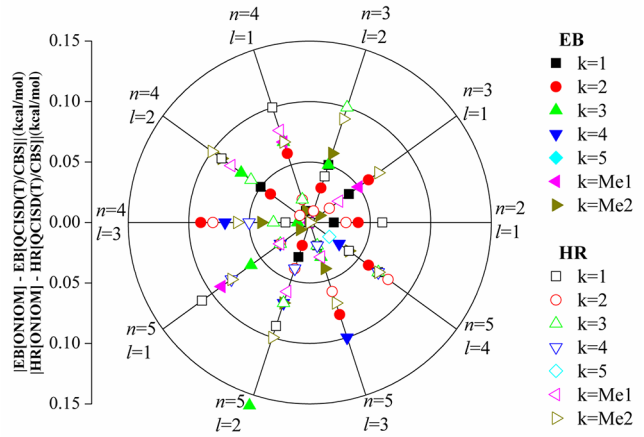

Figure 5. Difference (in absolute value) of the calculated energy barriers, EB[ONIOM] − EB[QCISD(T)/CBS] (denoted by the solid symbols), and that of the calculated heat of reactions, HR[ONIOM] − HR[QCISD(T)/CBS] (denoted by the open symbols), for the H attack reactions of $C_nH_{2n-1}COOCH_3$ + H (n = 2−5). The notation l (= 1−4) denotes the location of double bond from the closest to the farthest to the ester group, and k (= 1−5, Me1, and Me2) denotes the group under hydrogen attack. Me1 denotes the CH_3 in the alkyl chain, and Me2 denotes the CH_3 connected the alkoxy O atom.

where the EB difference is 0.17 kcal/mol. The slightly larger difference may be caused by the exclusion of the methoxy group from the CAP(2,2). According to the specification rules discussed in the preceding section, the CAP(2,2) for (13) includes three CH_2 groups and the carbonyl group. An extension of the CAP to include the whole ester group will diminish the difference.

DOI: 10.1021/acs.jpca.8b02327
J. Phys. Chem. A 2018, 122, 4882−4893

Table 2. Calculated EB and HR for Isomerization Reactions of $C_nH_{2n}COOCH_3$ (n = 2−5) with the ONIOM and QCISD(T)/CBS Methods[a]

	q = Me2	q = Me1	q = O	q = 2	q = 3	q = 4
C_3 (n = 2, p = 1)	31.68(31.68)/ 5.36(5.36)	40.17(40.14)/ 7.64(7.73)	41.59(41.59)/ 19.60(19.60)			
C_3 (n = 2, p = Me1)	23.66(23.66)/ −2.38(−2.38)		64.72(64.72)/ 11.87(11.87)			
C_4 (n = 3, p = 1)	31.22(31.22)/ 4.76(4.76)	41.85(41.81)/ 6.65(6.71)	39.82(39.82)/ 17.22(17.22)	37.55(37.51)/ 4.16(4.25)		
C_4 (n = 3, p = 2)	24.44(24.44)/ 0.52(0.52)	41.10(41.12)/ 2.49(2.46)	60.64(60.64)/ 12.97(12.97)			
C_4 (n = 3, p = Me1)	26.63(26.63)/ 1.95(1.95)					
C_5 (n = 4, p = 1)	31.20(31.20)/ 4.86(4.90)	26.59(26.55)/ 6.83(6.89)	42.31(42.31)/ 17.70(17.70)	37.73(37.68)/ 4.63(4.71)	39.62(39.55) /3.98(4.04)	
C_5 (n = 4, p = 2)	23.55 (23.55)/ 0.19(0.19)	41.41(41.40)/ 2.20(2.18)	60.57(60.57)/ 12.99(12.99)		39.38(39.40) /−0.64(−0.67)	
C_5 (n = 4, p = 3)	25.43(25.43)/ 0.86(0.86)	40.79(40.81)/ 2.90(2.85)				
C_5 (n = 4, p = Me1)	23.79(23.79)/ −1.99(−1.99)					
C_6 (n = 5, p = 1)	31.20(31.18)/ 4.89(4.93)	19.73(19.66)/ 6.66(6.72)	42.32(42.28)/ 17.63(17.61)	37.69(37.61) /4.67(4.74)	39.27(39.19) /4.35(4.40)	24.00(23.90) /4.08(4.13)
C_6 (n = 5, p = 2)	23.84(23.80)/ 0.19(0.19)	25.41(25.39)/ 2.00(1.98)	60.54(60.54)/ 12.92(12.87)		39.36(39.38) /−0.31(−0.34)	39.95(39.93) /−0.58(−0.61)
C_6 (n = 5, p = 3)	24.91(24.91)/ 0.53(0.53)	40.89(40.85)/ 2.35(2.31)				38.93(38.97) /−0.24(−0.27)
C_6 (n = 5, p = 4)	25.59(25.59)/ 0.80(0.80)	40.74(40.74)/ 2.58(2.58)				
C_6 (n = 5, p = Me1)	25.12(25.12)/ −1.79(−1.79)					

[a]The notation p (= 1−4) denotes the possible radical location in the reactant, and q (= 1−4) denotes the possible location in the product from the closest to the farthest to the ester group. Me1 denotes the CH_3 in the alkyl chain, and Me2 denotes the CH_3 connected the alkoxy O atom (denoted by O). Each item reads as EB by the ONIOM method (EB by the QCISD(T)/CBS method)/HR by the ONIOM method (HR by the QCISD(T)/CBS method). Empty cells correspond to those nonexistent reactions.

3.1.2. Isomerization Reactions. The predicted energies by using the ONIOM[QCISD(T)/CBS:DFT] and QCISD(T)/CBS methods for the isomerization reactions of $C_nH_{2n}COOCH_3$ (n = 2−5) are presented in Table 2. All the possible active sites of the radical locations in the reactants and products were considered for a systematical and comprehensive validation. The notation p (= 1−4, Me1, and Me2) denotes the radical location in the reactant and q (= 1−4, Me1, Me2, and O) in the product. Me1 denotes the CH_3 in the alkyl chain, and Me2 denotes the CH_3 connected the alkoxy O atom (denoted by O). The empty cells in Table 2 correspond to those nonexistent reactions.

All the calculated EB[ONIOM] (or HR[ONIOM]) are in excellent agreement with EB[QCISD(T)/CBS] (or HR-[QCISD(T)/CBS]) with the absolute differences being all less than 0.10 kcal/mol, as shown in Figure 6 for illustration. Note that the CAP(2,2) for these isomerization reactions includes all the atoms within the ring-structure of transition state. For those larger methyl esters such as methyl oleate to be discussed in Section 5, the transition states may have to be dealt with at different levels, and larger discrepancies may be therefore caused.

3.1.3. β-Scission Reactions. The predicted energies by using the ONIOM[QCISD(T)/CBS:DFT] and QCISD(T)/CBS methods for the β-scission reactions of $C_nH_{2n}COOCH_3$ (n = 2−5) are presented in Table 3. All the possible radical locations in the reactants were considered for a systematical and

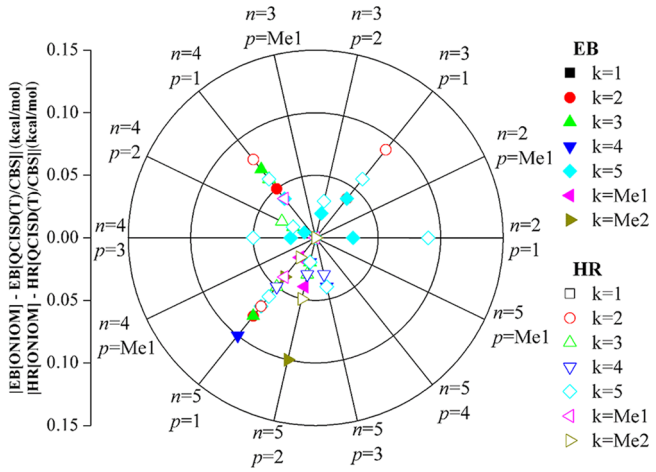

Figure 6. Difference (in absolute value) of the calculated energy barriers, EB[ONIOM] − EB[QCISD(T)/CBS] (denoted by the solid symbols), and that of the calculated heat of reactions, HR[ONIOM] − HR[QCISD(T)/CBS] (denoted by the open symbols), for the isomerization reactions of $C_nH_{2n}COOCH_3$ (n = 2−5). The notation p (= 1−4, Me1, and Me2) denotes the possible radical location in the reactant, and q (= 1−4, Me1, Me2, and O) denotes the possible radical location in the product. Me1 denotes the CH_3 in the alkyl chain, and Me2 denotes the CH_3 connected to the alkoxy O atom (denoted by O).

DOI: 10.1021/acs.jpca.8b02327
J. Phys. Chem. A 2018, 122, 4882−4893

Table 3. Calculated EB and HR for β-Scission Reactions of $C_nH_{2n}COOCH_3$ (n = 2−5) with the ONIOM and QCISD(T)/CBS Methods[a]

	p = Me2	p = Me1	p = O	p = 1	p = 2	p = 3	p = 4
C_3 (n = 2)	32.16(32.16)/	31.97(31.97)/	22.57(22.57)/	52.11(52.11)/			
	21.32(21.32)	26.93(26.93)	−1.31(−1.31)	50.14(50.14)			
C_4 (n = 3)	32.18(32.24)/	26.28(26.16)/	21.07(21.07)/	51.37(51.37)/			
	21.24(21.30)	19.56(19.63)	−3.53(−3.53)	49.39(49.39)			
C_4 (n = 3)	32.18(32.24)/	26.28(26.16)/	21.07(21.07)/	32.44(32.46)/			
	21.24(21.30)	19.56(19.63)	−3.53(−3.53)	26.98(27.04)			
C_5 (n = 4)	31.80(31.90)/	30.73(30.75)/	21.08(21.08)/	51.18(51.24)/	31.30(31.30)/	25.72(25.56)/	
	20.78(20.84)	23.46(23.50)	−3.41(−3.41)	49.35(49.36)	27.49(27.49)	19.94(20.03)	
C_5 (n = 4)	31.80(31.90)/	30.73(30.75)/	37.06(36.96)/	31.09(31.08)/	31.16(31.18)/	25.72(25.56)/	
	20.78(20.84)	23.46(23.50)	30.02(30.07)	26.53(26.61)	23.08(23.06)	19.94(20.03)	
C_6 (n = 5)	31.87(31.95)/	30.35(30.30)/	20.89(21.02)/	51.22(51.26)/	31.19(31.16)/	30.84(30.80)/	30.66(30.66)/
	20.82(20.88)	22.62(22.61)	−3.47(−3.43)	49.46(49.46)	27.48(27.47)	22.61(22.54)	23.82(23.87)
C_6 (n = 5)	31.87(31.95)/	30.35(30.30)/	35.67(35.67)/	31.68(31.67)/	30.17(30.19)/	25.83(25.66)/	30.66(30.66)/
	20.82(20.88)	22.62(22.61)	29.62(29.62)	27.62(27.70)	22.51(22.50)	20.16(20.25)	23.82(23.87)

[a]The notation p(= 1−4) denotes the possible radical location in the reactant from the closest to the farthest to the ester group. Me1 denotes the CH_3 in the alkyl chain, and Me2 denotes the CH_3 connected to the alkoxy O atom (denoted by O). Each item reads as EB by the ONIOM method (EB by the QCISD(T)/CBS method)/HR by the ONIOM method (HR by the QCISD(T)/CBS method). Empty cells correspond to those nonexistent reactions.

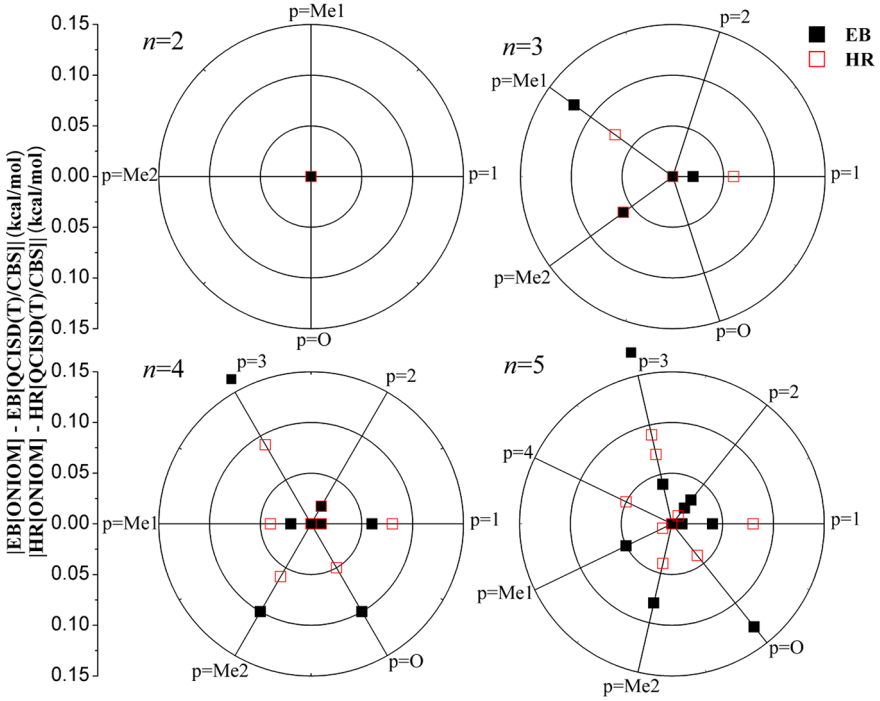

Figure 7. Difference (in absolute value) of the calculated energy barriers, EB[ONIOM] − EB[QCISD(T)/CBS] (denoted by the solid symbols), and that of the calculated heat of reactions, HR[ONIOM] − HR[QCISD(T)/CBS] (denoted by the open symbols), for the β-scission reactions of $C_nH_{2n}COOCH_3$ (n = 2−5). The notation p (= 1−4, Me1, Me2, and O) denotes the radical location in the reactant from the closest to the farthest to the ester group. Me1 denotes the CH_3 in the alkyl chain, and Me2 denotes the CH_3 connected to the alkoxy O atom (denoted by O).

comprehensive validation. The notation p (= 1−4, Me1, Me2, and O) denotes the possible radical location from the closest to the farthest to the ester group. Me1 denotes the CH_3 in the alkyl chain, and Me2 denotes the CH_3 connected to the alkoxy O atom (denoted by O). The empty cells in Table 3 correspond to the nonexistent reactions.

As shown in Figure 7, almost all the absolute differences are less than 0.15 kcal/mol, which again substantiates the accuracy of the present ONIOM method. There exist two exceptional cases: the EBs for (n = 4, p = 3)

$$CH_3C{\cdot}H(CH_2)_2COOCH_3 \rightarrow CH_3CH{=}CH_2 + {\cdot}CH_2COOCH_3 \quad (14)$$

and (n = 5, p = 3)

$$CH_3CH_2C{\cdot}H(CH_2)_2COOCH_3 \rightarrow {\cdot}CH_3 + CH_2{=}CH(CH_2)_2COOCH_3 \quad (15)$$

which have slightly larger differences than 0.15 kcal/mol by 0.01 and 0.02 kcal/mol, respectively. In both cases, the CAP(2,2) excludes the methyl group connected to the ester group. Slightly

DOI: 10.1021/acs.jpca.8b02327
J. Phys. Chem. A 2018, 122, 4882−4893

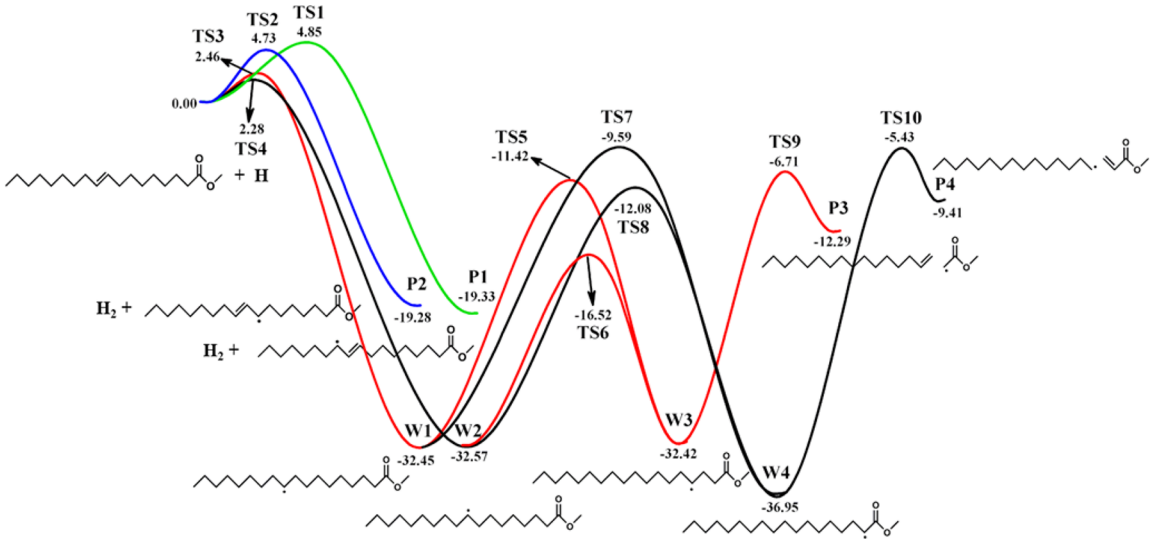

Figure 8. Energetically favorable pathways on the PES of $CH_3(CH_2)_7CH{=}CH(CH_2)_7COOCH_3$ at the ONIOM[QCISD(T)/CBS:DFT]//B3LYP/6-311++G(d,p) level.

Table 4. Calculated EB and HR for the Energetically Favorable Reactions between $CH_3(CH_2)_7CH{=}CH(CH_2)_7COOCH_3$ and Hydrogen Radical with the ONIOM Method[a]

H attack reaction	k = Me1	k = Me2	k = 1	k = 2	k = 3	k = 4	k = 5	k = 6	k = 7
C_{18} (n = 17, l = 8)	10.03/	10.39/	7.07/	8.10/	7.36/	7.60/	7.31/	7.72/	4.73/
	−3.73	−5.53	−10.56	−5.72	−6.00	−6.08	−6.10	−5.87	−19.28
	k = 8	k = 9	k = 10	k = 11	k = 12	k = 13	k = 14	k = 15	k = 16
C_{18} (n = 17, l = 8)	2.46/	2.28/	4.85/	7.45/	7.39/	7.26/	7.27/	7.25/	7.40/
	−32.45	−32.57	−19.33	−5.80	−6.09	−6.11	−6.06	−6.17	−6.42
isomerization	q = 1	q = 3		q = 1	q = 3				
C_{18} (n = 17, p = 8)	20.49/	16.05/	C_{18} (n = 17, p = 9)	22.86/	21.03/				
	−4.38	0.15		−4.50	0.03				
β-scission	q = 1	q = 3							
C_{18} (n = 17, p = 3)	25.71/	31.52/							
	20.13	27.54							

[a]The notation p (= 1−4) denotes the radical location in the reactant, and q = 1−4 denotes the location in the product from the closest to the farthest to the ester group. Me1 denotes the CH_3 in the alkyl chain, and Me2 denotes the CH_3 connected the alkoxy O atom (denoted by O). The notation l = 8 denotes the location of the double bond from the ester group, k (= 1−16, Me1, Me2) denotes the group under hydrogen attack, p = 3, 8, 9 indicates the radical location in the reactant, and q = 1, 3 denotes the location in the product. Me1 denotes the CH_3 in the alkyl chain, and Me2 denotes the CH_3 connected to the alkoxy O atom.

increasing the CAP to include the methyl group will vanish the differences.

3.2. PES and ONIOM Energies of $CH_3(CH_2)_7CH{=}CH(CH_2)_7COOCH_3$ + H. The present ONIOM method was applied to a substantially larger and practically useful system: the reactions between methyl oleate with a hydrogen radical, $CH_3(CH_2)_7CH{=}CH(CH_2)_7COOCH_3$ + H. Methyl oleate has only one C=C double bond (between No. 8 and No. 9 CH groups) in the molecule. According to the present notation, the reaction system corresponds to the case of $C_nH_{2n-1}COOCH_3$ + H (n = 17, l = 8). The PES of $CH_3(CH_2)_7CH{=}CH(CH_2)_7COOCH_3$ + H was studied at the level of ONIOM-[QCISD(T)/CBS:DFT]//B3LYP/6-311++G(d,p). For clarity and simplicity, only energetically favorable pathways, whose EBs are lower than 5 kcal/mol for hydrogen abstraction reactions and lower than 30 kcal/mol for isomerization reactions, are shown in Figure 8.

The predicted ONIOM energies for all the possible hydrogen abstraction and addition reactions are presented in Table 4. Several observations can be made from these results. First, the hydrogen abstraction reactions from two methyl groups (i.e., k = Me and 17) have the highest energy barriers, which are ~10 kcal/mol and consistent with those similar reactions for $C_{15}H_{31}COOCH_3$ + H. Second, the hydrogen abstraction reactions from a CH_2 group (i.e., k = 1−6 and 11−16) other than the two immediately adjacent to the C=C double bond have energy barriers of ~7 kcal/mol, which are again consistent with those reactions for $C_{15}H_{31}COOCH_3$ + H.

The hydrogen abstraction reactions from the No. 7 and No. 10 CH_2 groups, which are close to the C=C double bond, are as follows.

$$CH_3(CH_2)_7CH{=}CH(CH_2)_7COOCH_3 + H\cdot \rightarrow CH_3(CH_2)_7CH{=}CHC\cdot H(CH_2)_6COOCH_3(P1) + H_2 \quad (16)$$

$$CH_3(CH_2)_7CH{=}CH(CH_2)_7COOCH_3 + H\cdot \rightarrow CH_3(CH_2)_6C\cdot HCH{=}CH(CH_2)_7COOCH_3(P2) + H_2 \quad (17)$$

DOI: 10.1021/acs.jpca.8b02327
J. Phys. Chem. A 2018, 122, 4882−4893

whose energy barriers of 4.85 and 4.73 kcal/mol are lower than other hydrogen abstraction channels due to the conjugation effect of the C═C double bond.

The hydrogen addition reactions to the C═C double bond (i.e., to either No. 8 or No. 9 CH group) are as follows.

$$CH_3(CH_2)_7CH{=}CH(CH_2)_7COOCH_3 + H\cdot \rightarrow CH_3(CH_2)_7C\cdot HCH_2(CH_2)_7COOCH_3\ (W1) \quad (18)$$

$$CH_3(CH_2)_7CH{=}CH(CH_2)_7COOCH_3 + H\cdot \rightarrow CH_3(CH_2)_7CH_2C\cdot H(CH_2)_7COOCH_3\ (W2) \quad (19)$$

whose energy barriers of 2.28 and 2.46 kcal/mol are the lowest on the PES so that their subsequent reactions should be taken into account.

The complex W1 can isomerize to W3 via a transition state that has an eight-member ring structure:

$$CH_3(CH_2)_7C\cdot HCH_2(CH_2)_7COOCH_3\ (W1) \rightarrow CH_3(CH_2)_{13}C\cdot H(CH_2)_2COOCH_3\ (W3) \quad (20)$$

The CAP(2,2) for the isomerization reaction 20 consists of 11 non-hydrogen atoms. The product of reaction 20, namely, the complex W3, can subsequently undergo β-scission as follows

$$CH_3(CH_2)_{13}C\cdot H(CH_2)_2COOCH_3\ (W3) \rightarrow CH_3(CH_2)_{13}CH{=}CH_2 + C\cdot H_2COOCH_3\ (P3) \quad (21)$$

which has the lowest energy barrier among all the β-scission reactions under consideration because of the conjugation effect in the W4, which makes the biomolecular products more stable and the reaction more energetically favorable.

The complex W1 can also isomerize to W4 via a transition state that has a 10-member-ring structure

$$CH_3(CH_2)_7C\cdot HCH_2(CH_2)_7COOCH_3\ (W1) \rightarrow CH_3(CH_2)_{15}C\cdot HCOOCH_3\ (W4) \quad (22)$$

The CAP(2,2) for the reaction consists of 12 non-hydrogen atoms. The product of reaction 22, namely, the complex W4, can undergo β-scission as follows

$$CH_3(CH_2)_{15}C\cdot HCOOCH_3\ (W4) \rightarrow CH_3(CH_2)_{13}C\cdot H_2 + CH_2{=}CHCOOCH_3\ (P4) \quad (23)$$

which has the energy barrier slightly higher than that for (21) and constitutes another energetically favorable reaction pathway.

Similarly, the complex W2 undergoes isomerization reactions to form W3 or W4 as follows:

$$CH_3(CH_2)_7CH_2C\cdot H(CH_2)_7COOCH_3\ (W2) \rightarrow CH_3(CH_2)_{13}C\cdot H(CH_2)_2COOCH_3\ (W3) \quad (24)$$

$$CH_3(CH_2)_7CH_2C\cdot H(CH_2)_7COOCH_3\ (W2) \rightarrow CH_3(CH_2)_{15}C\cdot HCOOCH_3\ (W4) \quad (25)$$

There are no thermochemical data obtained by high-level theoretical methods for these large unsaturated esters in the literature. Therefore, the direct validation of these energies predications is unavailable up to now. The corresponding energies shown in Table 4 are believed to be reasonable and accurate, since the proposed ONIOM method has been extensively validated.

It is noted that the conformational flexibility of large molecules increases at high temperatures, which may lead to the emergence of other reaction channels by the mechanisms such as "well merging" and "well skipping"[38,39] on the PES. However, in the present study, we focused on comparing different electronic structure methods for high-level single-point energy calculations, and the chemical kinetics of the studied reactions will be considered in our future work. The proposed ONIOM method can be used to provide accurate energies, which are key parameters for a chemical kinetics study. So the present conclusions are not affected by the possible emergence of other reaction channels.

As an important issue of the present study, we compared the computational costs of the ONIOM method and the QCISD(T)/CBS method for representative cases, as shown in Table S1 in the Supporting Information. It is seen that most of the computation time for each case was spent on the QCISD(T)/cc-pVTZ calculation. In the present ONIOM calculations with CAP(2,2), the number of non-hydrogen atoms included in the high layer is always 5−7 and does not increase with the size of molecules. Consequently, the computational load of the present ONIOM method remains to be equivalent to that of QCISD(T)/cc-pVTZ for a system containing 5−7 non-hydrogen atoms. Overall, the ONIOM method can reduce the computational load by ∼1 order of magnitude for the present reaction systems.

4. CONCLUDING REMARKS

An ONIOM[QCISD(T)/CBS:DFT] method was proposed and systematically validated in the present computational work for the hydrogen abstraction, the hydrogen addition, the isomerization, and the β-scission reactions between unsaturated methyl esters $C_nH_{2n-1}COOCH_3$ (n = 2−5, 17) and a hydrogen radical. This study further substantiates the computational accuracy and efficiency of the proposed ONIOM method, which has already been sufficiently verified in the previous study on the hydrogen abstraction reactions between saturated alkyl esters and hydrogen radical.

Because of the conjugation effect of the C═C double bond, the specification of CAP(2,2), which has been verified as the minimally required chemically active portion for the ONIOM method, for various types of reaction can be summarized in the following rules:

Rule (i): CAP(2, 2) is uniformly composed of the chemically active centers, referred to as CAC(s), and the two adjacent groups on each side of the CAC(s). The components of the CAC(s) vary for different types of reaction.

Rule (ii): For the hydrogen addition reactions, the CAC is the CH group under attack by the hydrogen atom.

Rule (iii): For the hydrogen abstraction reactions from the CH_2 (or CH_3) group that are not immediately adjacent to the C═C double bond, the specification of the CAC is the same as that for $C_nH_{2n+1}COOCH_3$ + H—the CAC is the CH_2 (or CH_3) group under attack by the hydrogen atom.

Rule (iv): For the hydrogen abstraction reactions from the CH_2 (or CH_3) group that are immediately adjacent to the C═C double bond, the CAC should include the double bond to account for the conjugation effect.

Rule (v): For the isomerization reactions of the radical products from the reactions concerned in Rules (ii)−(iv), two CACs are needed, with one being the CH_2 (CH_3) yielding the

DOI: 10.1021/acs.jpca.8b02327
J. Phys. Chem. A 2018, 122, 4882−4893

hydrogen atom and the other being the CH group receiving the hydrogen atom.

Rule (vi): For the β-scission reactions of the radical products from the reactions concerned in Rules (ii)−(iv), the CAC consists of the radical site and its adjacent α and β groups.

Rule (vii): In general, a CAP(2,2) includes only two neighboring groups from each side of its CAC. Functional groups are always included in the CAP if any of these neighboring groups are a part of the functional groups.

The accuracy of calculated ONIOM[QCISD(T)/CBS:DFT] energies have been validated by comparing with the QCISD(T)/CBS energies, and almost all the energy differences between these two methods are less than 0.15 kcal/mol. In addition, the ONIOM method was used to identify the energetically favored reaction pathways on the PES of $CH_3(CH_2)_7CH{=}CH(CH_2)_7$-$COOCH_3$ + H. The energy barriers of H addition reactions are lower than H abstraction reactions with mean difference of ∼5 kcal/mol. Overall, the present ONIOM[QCISD(T)/CBS:DFT] method provides a computationally accurate and affordable approach to study the large unsaturated alkyl esters that are of great interest to combustion chemistry.

■ ASSOCIATED CONTENT

Supporting Information

The Supporting Information is available free of charge on the ACS Publications website at DOI: 10.1021/acs.jpca.8b02327.

Optimized geometries at the B3LYP/6-311++G(d,p) level for all the stationary points on the potential energy surfaces (PDF)

■ AUTHOR INFORMATION

Corresponding Author

*E-mail: pengzhang.zhang@polyu.edu.hk. Fax: (852)23654703. Phone: (852)27666664.

ORCID

Lidong Zhang: 0000-0002-4924-1927

Notes

The authors declare no competing financial interest.

■ ACKNOWLEDGMENTS

This work was supported partly by NSFC (91641105) and partly by the Hong Kong RGC/ECS (PolyU 5380/13E) and SRFDP & GRC ERG Joint Research Scheme (M-PolyU509/13). L.Z. was additionally supported by National Key Scientific Instruments and Equipment Development Program of China (2012YQ22011305) and NSFC (51676176).

■ REFERENCES

(1) Lin, L.; Cunshan, Z.; Vittayapadung, S.; Xiangqian, S.; Mingdong, D. Opportunities and challenges for biodiesel fuel. *Appl. Energy* **2011**, *88* (4), 1020−1031.

(2) Demirbas, A. Importance of biodiesel as transportation fuel. *Energy Policy* **2007**, *35* (9), 4661−4670.

(3) Pienkos, P. T.; Darzins, A. The promise and challenges of microalgal - derived biofuels. *Biofuels, Bioprod. Biorefin.* **2009**, *3* (4), 431−440.

(4) Ma, F.; Hanna, M. A. Biodiesel production: a review. *Bioresour. Technol.* **1999**, *70* (1), 1−15.

(5) Bounaceur, R.; Warth, V.; Sirjean, B.; Glaude, P.-A.; Fournet, R.; Battin-Leclerc, F. Influence of the position of the double bond on the autoignition of linear alkenes at low temperature. *Proc. Combust. Inst.* **2009**, *32* (1), 387−394.

(6) Coniglio, L.; Bennadji, H.; Glaude, P. A.; Herbinet, O.; Billaud, F. Combustion chemical kinetics of biodiesel and related compounds (methyl and ethyl esters): Experiments and modeling−Advances and future refinements. *Prog. Energy Combust. Sci.* **2013**, *39* (4), 340−382.

(7) Lai, J. Y.; Lin, K. C.; Violi, A. Biodiesel combustion: advances in chemical kinetic modeling. *Prog. Energy Combust. Sci.* **2011**, *37* (1), 1−14.

(8) Li, X.; You, X.; Law, C.; Truhlar, D. G. Kinetics and Branching Fractions of the Hydrogen Abstraction Reaction from Methyl Butenoates by H Atom. *Phys. Chem. Chem. Phys.* **2017**, *19*, 16563.

(9) Tan, T.; Yang, X.; Ju, Y.; Carter, E. A. Ab initio pressure-dependent reaction kinetics of methyl propanoate radicals. *Phys. Chem. Chem. Phys.* **2015**, *17* (46), 31061−31072.

(10) Thion, S.; Zaras, A. M.; Szori, M.; Dagaut, P. Theoretical kinetic study for methyl levulinate: oxidation by OH and CH3 radicals and further unimolecular decomposition pathways. *Phys. Chem. Chem. Phys.* **2015**, *17* (36), 23384−23391.

(11) Zhang, L.; Zhang, P. Towards high-level theoretical studies of large biodiesel molecules: an ONIOM [QCISD (T)/CBS: DFT] study of hydrogen abstraction reactions of C n H 2n+ 1 COOC m H 2m+ 1+ H. *Phys. Chem. Chem. Phys.* **2015**, *17* (1), 200−208.

(12) Dooley, S.; Curran, H. J.; Simmie, J. M. Autoignition measurements and a validated kinetic model for the biodiesel surrogate, methyl butanoate. *Combust. Flame* **2008**, *153* (1), 2−32.

(13) Fisher, E. M.; Pitz, W. J.; Curran, H. J.; Westbrook, C. K. Detailed chemical kinetic mechanisms for combustion of oxygenated fuels. *Proc. Combust. Inst.* **2000**, *28* (2), 1579−1586.

(14) Gaïl, S.; Thomson, M. J.; Sarathy, S. M.; Syed, S. A.; Dagaut, P.; Diévart, P.; Marchese, A. J.; Dryer, F. L. A wide-ranging kinetic modeling study of methyl butanoate combustion. *Proc. Combust. Inst.* **2007**, *31* (1), 305−311.

(15) Hakka, M. H.; Bennadji, H.; Biet, J.; Yahyaoui, M.; Sirjean, B.; Warth, V.; Coniglio, L.; Herbinet, O.; Glaude, P.-A.; Billaud, F.; et al. Oxidation of methyl and ethyl butanoates. *Int. J. Chem. Kinet.* **2010**, *42* (4), 226−252.

(16) Zhang, L.; Chen, Q.; Zhang, P. A theoretical kinetics study of the reactions of methylbutanoate with hydrogen and hydroxyl radicals. *Proc. Combust. Inst.* **2015**, *35* (1), 481−489.

(17) Westbrook, C. K.; Naik, C. V.; Herbinet, O.; Pitz, W. J.; Mehl, M.; Sarathy, S. M.; Curran, H. J. Detailed chemical kinetic reaction mechanisms for soy and rapeseed biodiesel fuels. *Combust. Flame* **2011**, *158* (4), 742−755.

(18) Sarathy, S. M.; Gail, S.; Syed, S. A.; Thomson, M. J.; Dagaut, P. A comparison of saturated and unsaturated C-4 fatty acid methyl esters in an opposed flow diffusion flame and a jet stirred reactor. *Proc. Combust. Inst.* **2007**, *31*, 1015−1022.

(19) Gaïl, S.; Sarathy, S. M.; Thomson, M. J.; Diévart, P.; Dagaut, P. Experimental and chemical kinetic modeling study of small methyl esters oxidation: Methyl (E)-2-butenoate and methyl butanoate. *Combust. Flame* **2008**, *155* (4), 635−650.

(20) Bax, S.; Hakka, M. H.; Glaude, P. A.; Herbinet, O.; Battin-Leclerc, F. Experimental study of the oxidation of methyl oleate in a jet-stirred reactor. *Combust. Flame* **2010**, *157* (6), 1220−1229.

(21) Herbinet, O.; Pitz, W. J.; Westbrook, C. K. Detailed chemical kinetic mechanism for the oxidation of biodiesel fuels blend surrogate. *Combust. Flame* **2010**, *157* (5), 893−908.

(22) Naik, C. V.; Westbrook, C. K.; Herbinet, O.; Pitz, W. J.; Mehl, M. Detailed chemical kinetic reaction mechanism for biodiesel components methyl stearate and methyl oleate. *Proc. Combust. Inst.* **2011**, *33*, 383−389.

(23) Bennadji, H.; Coniglio, L.; Billaud, F.; Bounaceur, R.; Warth, V.; Glaude, P. A.; Battin-Leclerc, F. Oxidation of Small Unsaturated Methyl and Ethyl Esters. *Int. J. Chem. Kinet.* **2011**, *43* (4), 204−218.

(24) Yang, B.; Westbrook, C. K.; Cool, T. A.; Hansen, N.; Kohse-Hoinghaus, K. Photoionization mass spectrometry and modeling study of premixed flames of three unsaturated C5H8O2 esters. *Proc. Combust. Inst.* **2013**, *34*, 443−451.

DOI: 10.1021/acs.jpca.8b02327
J. Phys. Chem. A 2018, 122, 4882−4893

(25) Zhang, Y.; Boehman, A. L. Autoignition of binary fuel blends of n-heptane and C-7 esters in a motored engine. *Combust. Flame* **2012**, *159* (4), 1619−1630.
(26) Westbrook, C. K.; Pitz, W. J.; Mehl, M.; Glaude, P. A.; Herbinet, O.; Bax, S.; Battin-Leclerc, F.; Mathieu, O.; Petersen, E. L.; Bugler, J.; Curran, H. J. Experimental and Kinetic Modeling Study of 2-Methyl-2-Butene: Allylic Hydrocarbon Kinetics. *J. Phys. Chem. A* **2015**, *119* (28), 7462−7480.
(27) Chang, Y. C.; Jia, M.; Li, Y. P.; Zhang, Y. Z.; Xie, M. Z.; Wang, H.; Reitz, R. D. Development of a skeletal oxidation mechanism for biodiesel surrogate. *Proc. Combust. Inst.* **2015**, *35*, 3037−3044.
(28) Wang, Q. D.; Zhang, W. D. Influence of the double bond on the hydrogen abstraction reactions of methyl esters with hydrogen radical: an ab initio and chemical kinetic study. *RSC Adv.* **2015**, *5* (84), 68314−68325.
(29) Westbrook, C. K.; Pitz, W. J.; Curran, H. J. Chemical kinetic modeling study of the effects of oxygenated hydrocarbons on soot emissions from diesel engines. *J. Phys. Chem. A* **2006**, *110* (21), 6912−6922.
(30) Zhang, K. W.; Togbe, C.; Dayma, G.; Dagaut, P. Experimental and kinetic modeling study of trans-methyl-3-hexenoate oxidation in JSR and the role of C═C double bond. *Combust. Flame* **2014**, *161* (3), 818−825.
(31) Papajak, E.; Truhlar, D. G. What are the most efficient basis set strategies for correlated wave function calculations of reaction energies and barrier heights? *J. Chem. Phys.* **2012**, *137* (6), 064110.
(32) Zhang, P.; Klippenstein, S. J.; Law, C. K. In *Ab Initio Kinetics for the Decomposition of α-Hydroxybutyl Radicals of n-Butanol;* Fall Technical Meeting of the Eastern States Section of the Combustion Institute; University of Connecticut, 2011.
(33) Lundberg, M.; Kawatsu, T.; Vreven, T.; Frisch, M. J.; Morokuma, K. Transition States in a Protein Environment − ONIOM QM:MM Modeling of Isopenicillin N Synthesis. *J. Chem. Theory Comput.* **2009**, *5* (1), 222−234.
(34) Livshits, E.; Baer, R. A well-tempered density functional theory of electrons in molecules. *Phys. Chem. Chem. Phys.* **2007**, *9* (23), 2932−2941.
(35) Sung, D. D.; Koo, I. S.; Yang, K.; Lee, I. DFT studies on the structure and stability of zwitterionic tetrahedral intermediate in the aminolysis of esters. *Chem. Phys. Lett.* **2006**, *426* (4), 280−284.
(36) Frisch, M. J.; Trucks, G. W.; Schlegel, H. B.; Scuseria, G. E.; Robb, M. A.; Cheeseman, J. R.; Scalmani, G.; Barone, V.; Mennucci, B.; Petersson, G. A.; Nakatsuji, H.; Caricato, M.; Li, X.; Hratchian, H. P.; Izmaylov, A. F.; Bloino, J.; Zheng, G.; Sonnenberg, J. L.; Hada, M.; Ehara, M.; Toyota, K.; Fukuda, R.; Hasegawa, J.; Ishida, M.; Nakajima, T.; Honda, Y.; Kitao, O.; Nakai, H.; Vreven, T.; Montgomery, J. A.; Peralta, J. E.; Ogliaro, F.; Bearpark, M.; Heyd, J. J.; Brothers, E.; Kudin, K. N.; Staroverov, V. N.; Keith, T.; Kobayashi, R.; Normand, J.; Raghavachari, K.; Rendell, A.; Burant, J. C.; Iyengar, S. S.; Tomasi, J.; Cossi, M.; Rega, N.; Millam, J. M.; Klene, M.; Knox, J. E.; Cross, J. B.; Bakken, V.; Adamo, C.; Jaramillo, J.; Gomperts, R.; Stratmann, R. E.; Yazyev, O.; Austin, A. J.; Cammi, R.; Pomelli, C.; Ochterski, J. W.; Martin, R. L.; Morokuma, K.; Zakrzewski, V. G.; Voth, G. A.; Salvador, P.; Dannenberg, J. J.; Dapprich, S.; Daniels, A. D.; Farkas, O.; Foresman, J. B.; Ortiz, J. V.; Cioslowski, J.; Fox, D. J. *Gaussian 09;* Gaussian, Inc.: Wallingford, CT, 2009.
(37) Van Gerpen, J.; Shanks, B.; Pruszko, R.; Clements, D.; Knothe, G. Biodiesel Production Technology. In *Subcontractor Report;* Prepared for National Renewable Energy Laboratory; Midwest Research Institute: Kansas City, MO, 2004.
(38) Miller, J. A.; Klippenstein, S. J. Master equation methods in gas phase chemical kinetics. *J. Phys. Chem. A* **2006**, *110* (36), 10528−10544.
(39) Georgievskii, Y.; Miller, J. A.; Burke, M. P.; Klippenstein, S. J. Reformulation and solution of the master equation for multiple-well chemical reactions. *J. Phys. Chem. A* **2013**, *117* (46), 12146−12154.

DOI: 10.1021/acs.jpca.8b02327
J. Phys. Chem. A 2018, 122, 4882−4893